Original paper

Gutenberg-Richter B Value Studies Along the Mexican Subduction Zone and Data Constraints

Lenin Ávila-Barrientos *[1] and F. Alejandro Nava Pichardo[2]

Received: February 24, 2020, accepted: July 7, 2020; online publication: October 1, 2020

Resumen

El valor b de la distribución Gutenberg-Richter es una de las herramientas más importantes para estudios de peligro sísmico; dicho valor es de gran utilidad para estimar razones de ocurrencia de sismos, y está relacionado también con niveles de esfuerzo del medio y presenta cambios precursores a la ocurrencia de grandes sismos. Sin embargo, determinaciones correctas y confiables del valor b dependen críticamente de contar con muestras suficientes. Llevamos a cabo estudios orientados a corroborar si efectivamente ocurren cambios precursores del valor b antes de sismos grandes ($M \geq 7.0$) a lo largo de la zona de subducción de México; estos estudios fueron basados en datos del catálogo del Servicio Sismológico Nacional (SSN) de 1988 a 2018. Lo resultados para cinco grandes sismos sugieren que los cambios precursores efectivamente existen, pero las diferencias entre los valores obtenidos no son estadísticamente significativas debido a las incertidumbres causadas porque el SSN usa diferentes escalas de magnitud para sismos pequeños (bajo M ~4.5) y para medianos a grandes (arriba de M ~4.5). Discutimos algunas limitaciones sobre la aplicabilidad de los datos del SSN.

Palabras clave: Peligro sísmico, Relación Gutenberg-Richter, SSN, Valor b, Zona de subducción Mexicana.

Abstract

The Gutenberg-Richter b value is one of the most important tools for seismic hazard studies; this value is most useful in estimating seismicity rates, and also is related to ambient stress levels and shows changes precursory to the occurrence of large earthquakes. However, correct and reliable determinations of the b value are critically dependent on having enough data samples. Studies oriented to corroborate whether precursory changes in the b value occur before large ($M \geq 7.0$) along the Mexican subduction zone, were done based on data from the Servicio Sismológico Nacional (SSN, Mexico's National Seismological Service) seismic catalog, from 1988 to 2018. Results for five earthquakes are suggestive that precursory changes may occur, but differences between measured values are not statistically significant because of large uncertainties due to the SSN using different magnitude scales for small (below M ~4.5) and medium to large (above M ~4.5) magnitudes. We discuss some limitations about the applicability of SSN data.

Keywords: b value, Gutenberg – Richter relation, Mexican subduction zone, Seismic hazard, SSN.

*Corresponding author: lenavila@cicese.mx

[1]Conacyt-CICESE, 22860, Ensenada, Baja California, México.

[2] CICESE, 22860, Ensenada, Baja California, México.

INTRODUCTION

The most common statistical tool for seismic hazard analysis is the Gutenberg – Richter (G-R) relation (Gutenberg and Richter, 1942, Ishimoto and Ida, 1939, Richter, 1958), that describes the distribution of earthquake magnitudes as

$$\log_{10} N(M) = a_1 - b(M - M_1) \ , \tag{1}$$

where N is the number of earthquakes with magnitude greater than or equal to M. Parameter a_1 is the logarithm of the total number of earthquakes with $M \geq M_1$, and parameter b, the slope of the relation commonly referred to as the b-value, is a measure of the relative quantities of small to large earthquakes and is usually ~1. M_1 (often denoted M_c) is the minimum magnitude for which coverage is complete, so that for smaller magnitudes $\log_{10} N$ and M are not linearly related.

While a_1 depends on the sample time and overall seismicity rate, b is related to the local geology and to the level of ambient stress (Scholz, 1968; Ghosh *et al.*, 2008) and is related to the fractality of fractures (Aki, 1981; Öncel *et al.*, 2001), so that it varies in time and space (Enescu and Ito, 2002). Several authors have found precursory changes in the b-value before the occurrence of major earthquakes (e.g. Shaw *et al.*, 1992; Wyss and Wiemer, 2000; Enescu and Ito, 2001; Márquez-Ramírez, 2012). Hence, b is an extremely important parameter in seismic hazard studies, both for estimating seismicity occurrence rates and as a precursor to large earthquakes.

There is no explicit upper limit to the magnitudes used in (1) and, since there must be a physical limit to how large an earthquake can be, many authors have proposed ways of truncating or modifying the G-R relation to account for a maximum possible magnitude M_{max} (Utsu, 1999). However, for most studies, the G-R relation ceases to be linear for magnitudes way below a maximum possible magnitude; obviously, magnitudes below that corresponding to $\log_{10}(M) < 0$ are either under- or over-sampled, but under- or over-sampling are common for magnitudes corresponding to $\log_{10}(M) < 0.5$ or 0.6. Let us denote by M_2 the magnitude above which over- or under-sampling occur, according to the completeness of the seismic catalog; then the G-R histogram will behave linearly only within the $[M_1, M_2]$ range.

Often the b-value is determined by fitting a straight line to the linear part of the G-R histogram that, since magnitudes are usually rounded to one decimal place, commonly has classes $\Delta M = 0.1$ wide.

Another common way to estimate the b-value is through the Aki-Utsu relation, which is based on the fact that the G-R relation (1) is a reverse cumulative distribution according to which magnitudes are distributed exponentially as

$$f(M) = \beta \, \mathrm{e}^{-\beta(M - M_1)}; \quad M \geq M_1, \tag{2}$$

where $\beta = b \ln(10)$. (c.f. Lomnitz, 1974), and β is related to the mean of the distribution, μ, as $\beta = 1/(\mu - M_1)$ (c.f. Parzen, 1960), so that

$$b = \frac{\log_{10} \mathrm{e}}{\mu - M_1} . \tag{3}$$

Aki (1965) showed that the maximum-likelihood estimate of *b*, b_m, is given by

$$b_m = \frac{\log_{10} e}{\bar{M} - M_1}, \tag{4}$$

where $\bar{M}$ is the sample mean, and Utsu (1965) pointed out that, since magnitudes are rounded to ΔM, the actual minimum magnitude is $M_1^U = M_1 - \Delta M / 2$, so that

$$b_m = \frac{\log_{10} e}{\bar{M} - M_1^U}. \tag{5}$$

Formula (5), which we will refer to as the Aki-Utsu estimate, has been widely used as a simple and straightforward way of estimating *b* directly from the magnitude sample mean, with no explicit need for a G-R histogram. However, in too many cases, people do not realize the need for correctly determining M_1^U, and of having a representative sample from the linear part of the histogram that is large enough so that $\bar{M} \cong \mu$, which is an absolute requirement for $b_m \cong b$. In too many cases $\bar{M}$ is estimated from too small samples, either because data are scarce or because no attention is paid to the matter of representativity, and small samples result in estimates with too much scatter to be useful (Kramer, 2014; Nava *et al.*, 2017a).

Whichever the method used to estimate the *b*-value, the data has to fulfill two requirements: first, the number of data in the $[M_1, M_2]$ range and the range itself need to be large enough so that a straight line can be adequately fitted or so that the observed mean magnitude is representative of the distribution mean; second, the data should be homogeneous.

The first requirement is not particularly difficult to meet when considering a large area or a long-time history, but when trying to have a good definition in time and/or space, which requires short time and/or space windows, then having a representative sample may be difficult.

The second requirement can have three aspects. Homogeneity in time: network coverage usually changes in time, but there are sophisticated techniques to deal, at least partially, with this aspect (e.g. Kijko, 2004; Kijko and Smit, 2014); also, *b* can change in time, in which case the measured value will be an average over time. Homogeneity in space: *b* does change from place to place so that a measure using data from a large region will yield a space average of the local values. Homogeneity in magnitude: it is not uncommon to report moment magnitudes for large earthquakes and use some other scale, such as coda or duration, for small and very small earthquakes; unless the small earthquake scale is correctly calibrated so that it measures like the large magnitude scale, then *b*-value determinations will be erroneous.

We next describe the problems encountered with this third requirement, while trying to determine whether changes in the *b*-value were observable before and after large earthquakes in the Mexican subduction zone.

The Mexican Subduction Zone

The tectonic activity in the south and southeast of México is governed by the subduction of the Rivera and Cocos plates under the North American plate (Figure 1). It is along this subduction zone where the largest earthquakes in Mexico have occurred. The subduction dip angle of the

Cocos plates changes from sub-horizontal below central México to major dip [25^0-30^0] near Chiapas to the southeast (Pérez-Campos *et al.*, 2008). The convergence velocity also changes, the Cocos plate has a velocity of 4 to 5 cm/yr in its western part, and the eastern part has velocity around 6 to 7 cm/yr relative to the North American plate (Dañobeitia *et al.*, 2016; Nuñez-Cornú *et al.*, 2016; Gutiérrez *et al.*, 2015; Kostoglodov and Bandy, 1995; Kostoglodov and Pacheco, 1999).

International catalogs do not list magnitudes small enough for reliable *b*-value determinations in this region, so that we decided to use data from the *Servicio Sismológico Nacional* (*SSN*, Mexico's National Seismological Service) seismic catalog, from 1988 (Zúñiga *et al.*, 2000) to 2019.

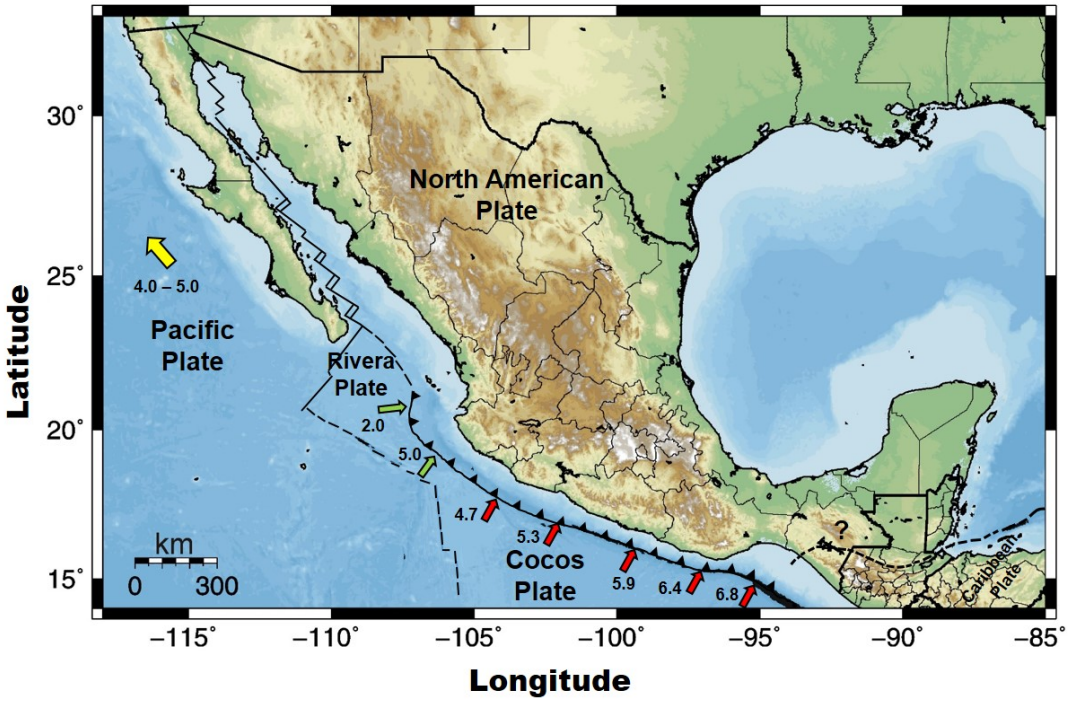

Figure 1. Tectonic plates interaction in México. Numbers indicate the velocity in cm/yr, and arrows show the local direction of the subducting plates relative to the North American plate. Red for the Cocos plate, Green for the Rivera plate, and Yellow for the Pacific plate.

Event Selection

We considered all earthquakes with $M \geq 7.0$ along the subduction zone, and selected a region around each mainshock, according to the spatial distribution of its aftershocks, to sample regions subject to the stresses that would cause the mainshock. Some of the regions were adjusted to avoid including events associated with another mainshock. Only mainshocks with enough data for pre- and post-event time windows were considered for *b* determination; Figure 2 shows the chosen areas, and Table 1 lists their magnitude, occurrence time, location, and the total number of events in window.

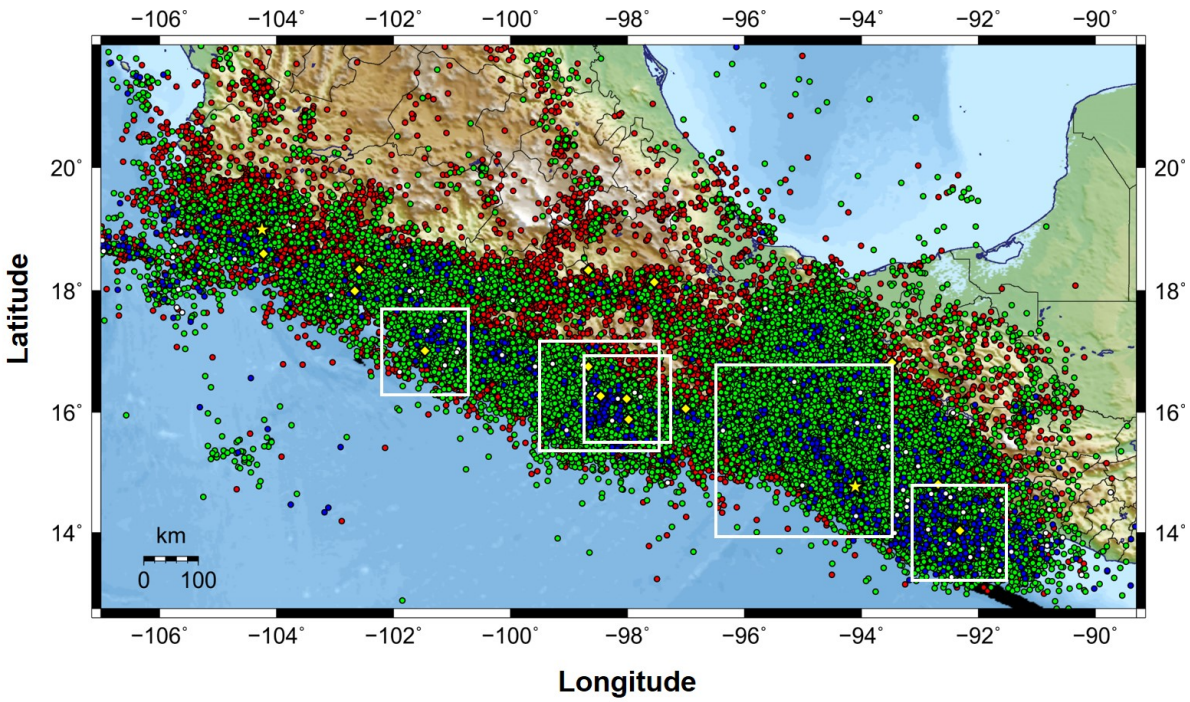

Figure 2. The squares indicate regions used for *b* value determination for large earthquakes along the Mexican subduction zone; from West to East: Guerrero 2014, Oaxaca 2012, Oaxaca 2018, Oaxaca-Chiapas 2017, Chiapas-Guatemala 2012. Dots represent epicenters: red $M < 4.0$, green $4.0 \leq M < 5.0$, blue $5.0 \leq M < 6.0$, grey $6.0 \leq M < 7.0$; Yellow diamond with $7.0 \leq M < 8.0$, and Yellow stars with $M \geq 8.0$.

The cumulative number of earthquakes curve for each region was plotted to determine times and threshold magnitudes for homogeneity; then, the cumulative curves were used to determine time windows. One of the time windows was chosen before the mainshock when stresses are expected to be high, and since the catalog does not extend backwards in time long enough to sample *b*-values before the stress build-up, in order to have a low-stress reference value, a second window was chosen after the mainshock liberated the stored stress and after the significant part of the aftershock activity, when seismicity was back to background level, so that we could sample low-stress *b*-values without aftershock noise.

As an example, Figure 3 shows the selection of pre and post-events for the 2012.85, *M* 7.3 earthquake located at the Mexico (State of Chiapas) — Guatemala border. From the cumulative curve for the whole region (Figure 3-Top), a clear change in the slope, possibly due to changes in the seismic network, is apparent around 2011, so that we used events from this point on to the end of the catalog. The pre- and post-mainshock time windows, which will be referred to as W1 and W2 from now on, are shown in Figure 3 (Bottom).

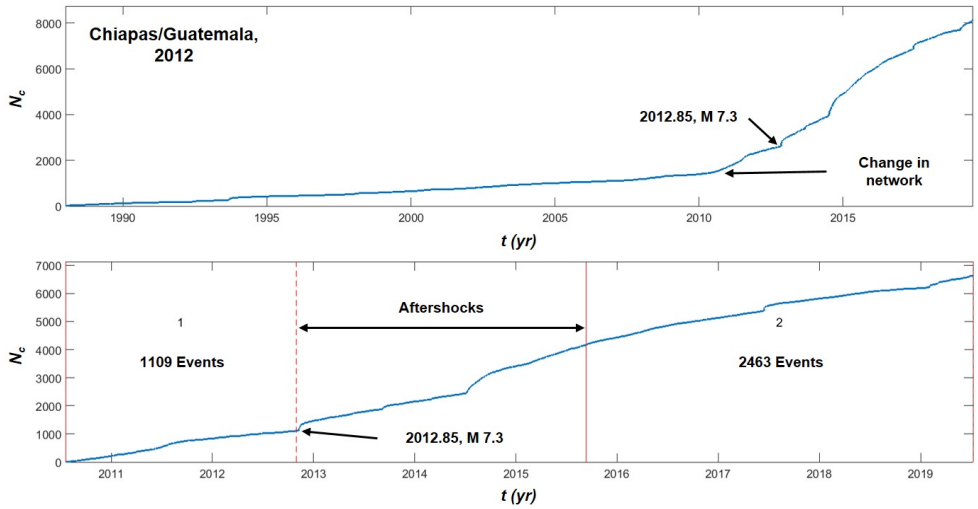

Figure 3. Cumulative curve for the 2012.85 earthquake located in the border of Chiapas/Guatemala. Top: Complete catalog. Bottom: Time windows, pre-earthquake W1 with 1109 events, and post-earthquake W2 with 2463.

B VALUE DETERMINATION METHOD AND DATA

We used the *most likely source b* method proposed by Nava *et al.* (2018). The M_1 and M_2 limits for the linear range of the G-R relation are chosen from the $\Delta M = 0.1$ G-R histogram, with the aid of the non-cumulative version of the histogram, and the Aki-Utsu method is used to estimate a *measured* b_m. Next, considering that the observed magnitudes constitute but one realization of random process having a source (or "true") value *b*, Monte Carlo methods are used to estimate the likelihood $\Pr(b_m \mid M_1, M_2, N, b)$, where N is the number of events in the $[M_1, M_2]$ range, for all different possible "true" *b*-values in a range around b_m which result in non-zero probabilities. For each possible source *b* value, N_r realizations of N events with magnitudes in the $[M_1, M_2]$ range are generated, from each realization a "measured" *b*-value is determined, and the number of times that this value equals b_m (number of "hits") is counted; a histogram of the number of hits for all source *b* values is made and normalized to result in a likelihood distribution. The *b*-value having the highest likelihood, b_x, is chosen as the most likely source *b*-value to have resulted in the observed realization. $N_r = 25{,}000$ Monte Carlo realizations were used here for each source *b* determination.

A further advantage of this method is that it gives the probability distribution for source *b*-values, so that it is possible to estimate bands for given confidence limits and estimate probabilities for two measures being distinct and the difference between them being significant.

RESULTS

Figure 3 shows the time window for the Chiapas-Guatemala 2012 earthquake; Figure 4 shows the windows selected for the rest of the earthquakes listed in Table 1. Because the aftershock sequence of the M_W 8.2 Oaxaca-Chiapas earthquake is not finished yet, it was not possible to have a post-quake window for this event.

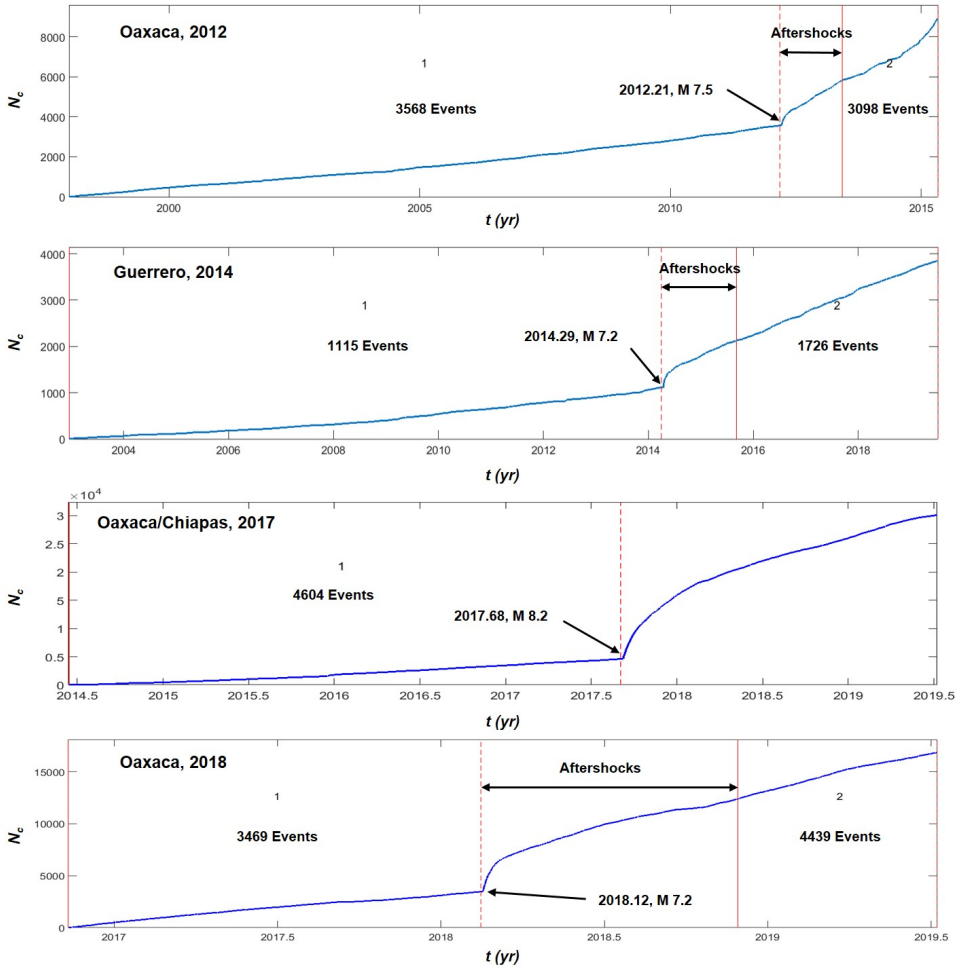

Figure 4. Pre and post-mainshock time windows for the earthquakes listed in Table 1.

Table 1.- Earthquakes with enough data for *b* determination.

M	Time	Lon	Lat	Depth	State Year	Total
7.50	2012.2179	-98.4570	16.2640	18.00	Oaxaca 2012	8927
7.30	2012.8516	-92.3160	14.0270	17.10	Chiapas/Guatemala 2012	6637
7.20	2014.2948	-101.4600	17.0110	18.00	Guerrero 2014	3857
8.20	2017.6855	-94.1030	14.7610	45.90	Oaxaca/Chiapas 2017	30143
7.20	2018.1287	-98.0140	16.2180	16.00	Oaxaca 2018	16833

Figures 5 to 9 show the fit of b_m to the G-R distribution (left), and the likelihood distribution and b_x choice (right) for events listed in Table 1; the b_m and b_x values are listed in Table 2.

Table 2. b-value before and after the large earthquakes.

Region	Time	*M*	Pre-event	Post-event

Event			b_m	b_x	M_1	M_2	N	b_m	b_x	M_1	M_2	N
Guerrero	2014.294	7.2	1.860	1.74	3.8	4.7	586	1.963	1.82	3.7	4.5	872
Oaxaca	2012.217	7.5	1.927	1.78	4.0	4.8	1200	2.550	2.41	3.7	4.3	1117
	2018.128	7.2	2.237	2.18	3.5	4.3	1485	2.437	2.26	3.6	4.2	1039
Oaxaca/ Chiapas	2017.685	8.2	2.388	2.18	3.9	4.5	914					
Chiapas/ Guatemala	2012.851	7.3	2.299	2.18	3.8	4.5	524	2.432	2.24	4.0	4.6	619

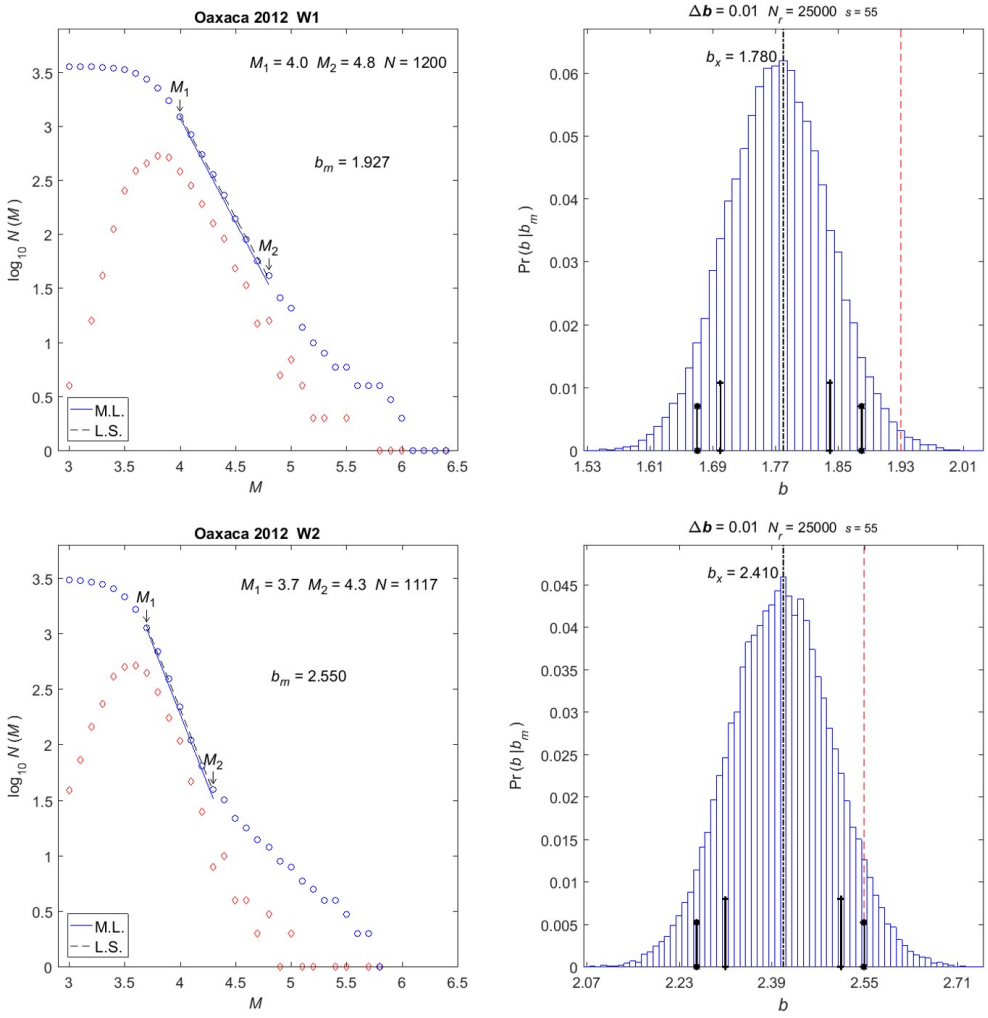

Figure 5. Oaxaca 2012. Left: G-R fit for b_m; (blue) circles are the G-R histogram, and (red) diamonds show the corresponding non-cumulative distribution; N is the number of data in the linear range from M_1 to M_2; M.L. is the straight line corresponding to b_m the maximum likelihood fit; L.S. is the dashed line for the least-squares fit (shown for comparison only). Right: b likelihood distribution; Δb is the class width, N_r is the number of Monte Carlo realizations, s is the pseudo-random number generator seed; the thin dashed red line indicates b_m, the black dash-dot line indicates b_x. Short vertical lines with crosses and asterisks indicate 75% and 90% confidence ranges, respectively. Top: Pre-event W1. Bottom: Post-event W2.

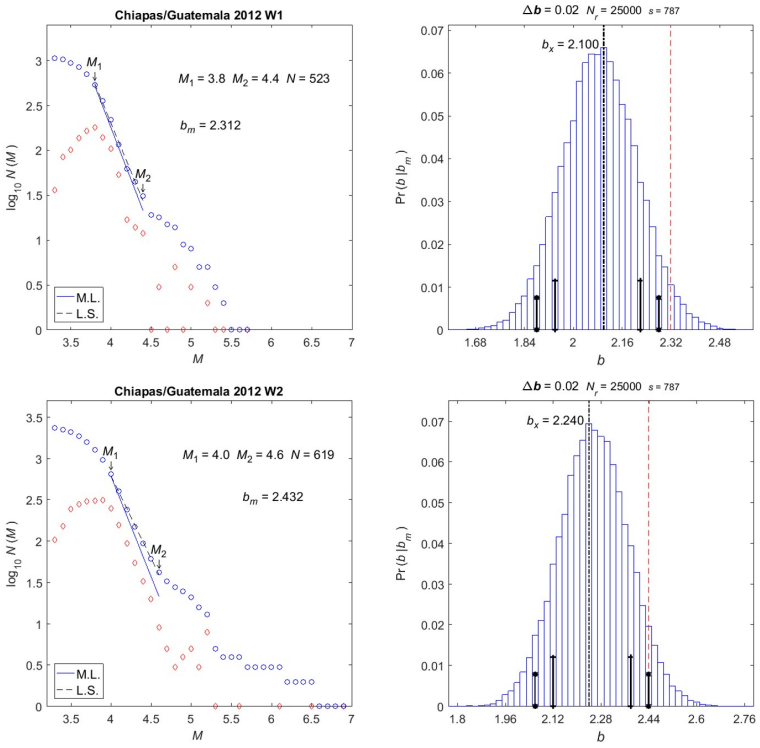

Figure 6. Chiapas-Guatemala 2012. Same conventions as in Figure 5.

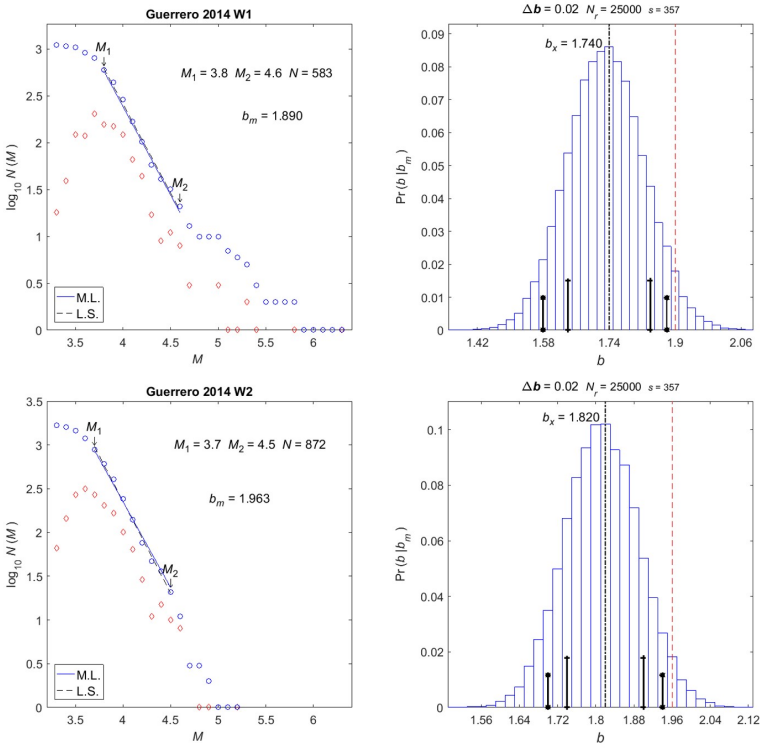

Figure 7. Guerrero 2014. Same conventions as in Figure 5.

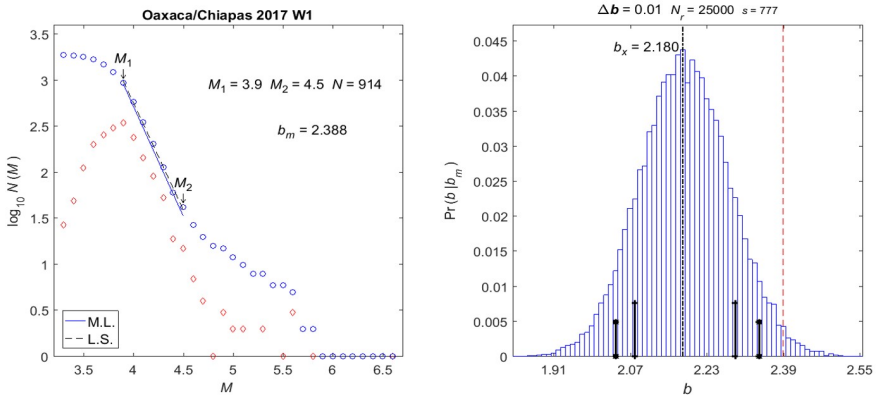

Figure 8. Oaxaca-Chiapas 2017. Same conventions as in Figure 5.

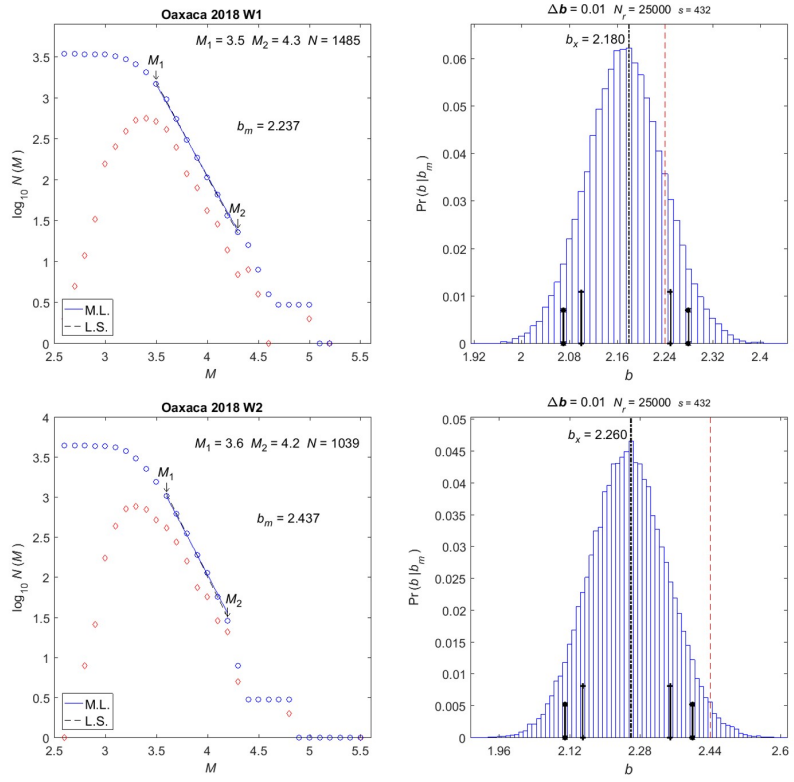

Figure 9. Oaxaca 2018. Same conventions as in Figure 5.

From these figures, it is clear that the G-R distributions do not have a single slope; all of them show a large slope for small magnitudes and a smaller one for larger magnitudes, meeting around magnitude 4.5. This feature is explained when topic *Mitos y Realidades*, in Sismos y Volcanes CDMX, mobile application software (2019), is consulted; the app. states that the SSN employs M_W for events larger than 4.5 and coda magnitude for events smaller than 4.5 (which scale is used for 4.5 magnitude events remains a mystery).

Because of this change in slope, it was not possible to obtain linear ranges over a wide enough magnitude interval; due to space and time limitations of the windows, only the small magnitude range was (barely) adequate for b_m estimation. As evidenced by the non-cumulative histograms

shown in the G-R plots, there were not enough data in the larger magnitudes range to obtain adequate estimates. Thus, we had to base our estimates on short ranges over only the smaller magnitudes.

A characteristic of the most likely source *b*-value method is that when the linear range is wide, some two or more magnitude units, say, and the number of data within the range is larger than about 2,000; the source *b* distributions are narrow and b_m and b_x are equal or differ by little. For the determinations presented here, with narrow ranges and few data, the source *b* distributions are wide.

We will now proceed to describe our results and defer their interpretation and assessment to the next section. The results are summarized in Table 2.

OAXACA 2012

Figure 5 shows that for this earthquake the linear magnitude range is short for both W1 and W2, so that b_x differs from b_m; for W1, the most likely source *b* value is $b_x = 1.78$, and the source *b* 90+% interval is [1.67, 1.88]; for W2, the most likely source *b* value is $b_x = 2.41$, and the source *b* 90+% confidence interval is [2.26, 2.55]; $\Delta b_x = 0.63$.

The number of data is large enough in both windows so that the source *b* distributions do not overlap; hence, we can say with certainty that the *b*-value before the mainshock is indeed smaller than for a low-stress regime, which reflects the stress accumulation leading to the mainshock and is thus an important observable with precursory value.

It may be argued that had a larger number of realizations or a different seed been used, the tails of the distributions could have been more extended; this is true, but since observed distributions have approximate Gaussian shapes, these extended tails will have extremely low probabilities, so that the probabilities on which significance estimates are based will remain essentially the same.

CHIAPAS-GUATEMALA 2012.

Data before and after this earthquake result in short G-R linear magnitude ranges (Figure 6, left), so that measured b_m values differ from the corresponding b_x ones. For W1, the most likely source b value is $b_x = 2.10$, and the source b 90+% interval is [1.88, 2.28]; for W2, the most likely source b value is $b_x = 2.24$, and the source b 90+% confidence interval is [2.06, 2.44].

From window W1 to window W2, there is an increase $\Delta b_x = 0.14$, but since the number of data in each window is rather small, the source b distributions are wide and overlap.

Let us denote the source b values in W1 by b_{W1}, and let the lower and upper limits of the W1 source b distribution by b_{11} and b_{12}, respectively, and let the corresponding values and limits for W2 be b_{W2}, b_{21} and b_{22} (we will use this notation henceforth). From the distribution histograms, the probability that b_{W1} takes values covered by the W2 distribution is $p_1 = \Pr(b_{W1} \geq b_{21})$, in this case $p_1 = 0.995337$; the probability that b_{W2} takes values covered by the W1 distribution is $p_2 = \Pr(b_{W2} \leq b_{12})$, in this case $p_2 = 0.997478$; the total probability that a source b value may belong to either distribution

is $p_{\cup} = p_1 + p_2 - p_1 p_2$, in this case $p_{\cup} = 0.999988$. Hence, we cannot reject the null hypothesis that b does not change with a certainty above $1 - p_{\cup} = 0.000012$.

GUERRERO 2014.

Results for this earthquake are similar to those for Chiapas-Guatemala 2012, with short linear G-R magnitude ranges and small quantities of data. For W1, the most likely source *b* value is $b_x = 1.74$, and the source *b* 90+% interval is [1.58, 1.88]; for W2, the most likely source *b* value is $b_x = 1.82$, and the source *b* 90+% confidence interval is [1.70, 1.94]; $\Delta b_x = 0.08$.

Overlap probabilities are $p_1 = 0.998962$ and $p_2 = 0.999970$ so that the null hypothesis probability is $p_{\cup} = 0.999999$; which means, that the possibility of b_x having the same value in both windows cannot be discarded.

OAXACA-CHIAPAS 2017.

As mentioned before, aftershocks of this M_W 8.2 do not allow for a W2 window; hence, we analyzed only a W1 window to see whether the measured values agreed with those for other earthquakes. Although the linear range was small, the number of data in it was intermediate. For this earthquake $b_x = 2.18$, and the source *b* 90+% confidence interval is [2.04, 2.34].

OAXACA 2018.

For W1, the most likely source *b* value is $b_x = 2.18$, and the source *b* 90+% interval is [2.07, 2.28]; for W2, the most likely source *b* value is $b_x = 2.26$, and the source *b* 90+% confidence interval is [2.11 2.40]; $\Delta b_x = 0.08$.

Overlap probabilities are $p_1 = 1.000000$ and $p_2 = 0.97164$ so that the null hypothesis probability is $p_{\cup} = 1.000000$.

DISCUSSION AND CONCLUSIONS

The change in slope around *M* 4.5 made it necessary to estimate *b* values using the smaller magnitudes only, and the measured *b*-values are larger than the semi-theoretical 1.5 maximum value (Olsson, 1999). These large values and the change in slope indicate that the M_c scale used by the SSN is not consistent with the M_W scale, so that the above mentioned maximum value does not apply to SSN small magnitudes. There were not enough data to obtain Aki-Utsu *b*-value estimates from the larger magnitudes, but least-squares fits (where possible for large magnitudes) yield values smaller than 1.5.

Hence, the *b*-values obtained here are useful only for comparisons among themselves, and cannot be used for comparisons with values obtained from data sets with true moment magnitudes.

The *b*-values for the Oaxaca 2012 earthquake are definitely smaller for the high stress regime before the mainshock than for the low-stress regime after it. Results for other earthquakes

consistently show *b*-values to be smaller before than after the main events, but the spreads in source *b* distributions make it impossible to discard the corresponding null hypotheses with any significant degree of confidence. We consider, however, that these results do strongly suggest smaller *b* values before the mainshocks than in low-stress regimes.

The question whether *b*-values are a useful precursor tool for the Mexican subduction zone remains an open question and will remain so until the SSN scales for small and large magnitudes agree (hopefully both scaling as M_W), so that reliable *b*-value determinations based on an appropriately wide magnitude range are possible. Meanwhile, let these observations be a caveat for researchers planning to work with *b*-values from the Mexican subduction zone.

ACKNOWLEDGMENTS

Many thanks to the SSN for their data, especially to Víctor Hugo Espíndola, and thanks to Antonio Mendoza for technical support. The Conacyt Cátedras program (2602) and project 222795 funded this research.

REFERENCES

Aki K., 1965, Maximum likelihood estimate of *b* in the formula *log(N) = a - bM* and its confidence limits. *Bulletin of the Earthquake Research Institute*, University of Tokyo 43, 237–239.

Aki K., 1981, A probabilistic synthesis of precursory phenomena, in Earthquake Prediction. An International Review, Maurice Ewing, (eds. D. W. Simpson. and P. G. Richards) American Geophysical Union, Washington, D. C. pp. 566–574.

Dañobeitia J., Bartolomé R., Prada M., Nuñez-Cornú F., Córdoba D., Bandy W. L., Estrada F., Cameselle A. L., Nuñez D., Castellón A., Alonso J. L., Mortera C., Ortiz M., 2016, Crustal Architecture at the Collision Zone Between Rivera and North American Plates at the Jalisco Block: Tsujal Project. *Pure and Applied Geophysics*. 173, 3553–3573. DOI 10.1007/s00024-016-1388-7

Enescu B., Ito K., 2001, Some premonitory phenomena of the 1995 Hyogo-Ken Nanbu (Kobe) earthquake: seismicity, b-value and fractal dimension. *Tectonophysics* 338, 297-314.

Enescu B., Ito K., 2002, Spatial analysis of the frequency-magnitude distribution and decay rate of aftershock activity of the 2000 Western Tottori earthquake. *Earth Planets Space* 54, 847-859.

Ghosh A., Newman A., Amanda M., Thomas A., Farmer G., 2008, Interface locking along the subduction megathrust from b value mapping near Nicoya Peninsula, Costa Rica. *Geophysical Research Letters*, 35, L01301. https://doi.org/10.1029/2007GL031617

Gutenberg B., Ritcher, C., 1942, Earthquake magnitude, intensity, energy and acceleration, *Bulletin of the Seismological Society of America*. Vol. 32, No. 3, pp 163-191.

Gutierrez Q. J., Escudero C. R., Núñez-Cornú F. J., 2015, Geometry of the Rivera-Cocos subduction zone inferred from local seismicity. *Bulletin of the Seismological Society of America*, 105(6), 3104–3113. DOI: 10.1785/012010358.

Ishimoto M., Iida K., 1939, Observations sur les seisms enregistrés par le microseismograph construit dernièrement (I), *Bulletin of the Earthquake Research Institute, University of Tokyo*, 17, 443-478.

Kijko A., 2004, Estimation of the maximum magnitude earthquake m_{max}. *Pure and Applied Geophysics*, 161, 1-27. DOI 10.1007/s00024-004-2531-4

Kijko A., Smit A., 2014, Extension of the Aki-Utsu b-value Parameter for incomplete Catalogues. Eurupean Geosciences Union, EGU2014-4959, Extreme events, multi-hazard and disaster risk assessment.

Kostoglodov V., Bandy W., 1995, Seismotectonic constraints on the convergence rate between the Rivera and North American plates. *Journal Geophysical Research*, 100, 17977–17989. DOI:10.1029/95JB01484.

Kostoglodov V., Pacheco J. F., 1999, Cien años de sismicidad en México. Instituto de Geofísica, UNAM.

Kramer Y., 2014, Minimum sample size for detection of Gutenberg-Richter's b-value. arXiv:1410.1815 [physics.geo-ph]

Lomnitz C., 1974, Global tectonics and earthquake risk. *Elsevier Scientific Publishing Company*, 320 pp.

Lomnitz-Adler J., Lomnitz C., 1979, A modified form of the Gutenberg-Richter magnitude-frequency relation. *Bulletin of the Seismological Society of America* 69: 1209-1214.

Márquez Ramírez V., 2012, *Análisis multifractal de la distribución espacial de sismicidad y su posible aplicación premonitora. Exploración de un posible mecanismo para la fractalidad mediante modelado semiestocástico*. PhD Thesis, Programa de Posgrado en Ciencias de la Tierra, Centro de Investigación Científica y de Educación Superior de Ensenada, Baja California, México.

Mitos y realidades, 2019, in Sismos y Volcanes CDMX for Apple IOS [Mobile application software]. Universidad Nacional Autónoma de México. Retrieved from Apple store. Consulted November 15, 2019.

Nava F. A., Márquez-Ramírez V. H., Zúñiga F. R., Ávila-Barrientos L., Quinteros C. B., 2017a, Gutenberg-Richter b-value maximum likelihood estimation and sample size. *Journal of Seismology*, 21, 127-135. https://doi.org/10.1007/s10950-016-9589-1

Nava F., Ávila-Barrientos L., Márquez-Ramírez V., Torres I., Zúñiga F., 2018, Sampling uncertainties and source b likelihood for the Gutenberg-Richter b-value from the Aki-Utsu method. *Journal of Seismology*, 22, 315-324. DOI: 10.1007/s10950-017-9707-8.

Núñez-Cornú J., Córdoba D., Dañobeitia J., Bandy W., Ortiz M., Figueroa B., Núñez D., Zamora-Camacho A., Espíndola J., Castellón A., Escudero C., Trejo-Gómez E., Escalona-Alcázar F., Suárez C., Nava F., Mortera C., TsuJal Working Group; 2016. Geophysical Studies across Rivera Plate and Jalisco Block, Mexico: TsuJal Project, *Seismological Research Letters*, DOI: 10.1785/0220150144

Olsson R., 1999, An estimation of the maximum b-value in the Gutenberg-Richter relation. *Geodynamics* 27, 547-552.

Öncel O. A., Wilson T. H., Nishizawa O., 2001, Size scaling relationships in the active fault networks of Japan and their correlation with Gutemberg-Richter b values. *Journal of Geophysical Research*, Vol. 106, No. B10, Pp. 21,827-21,841.

Pérez-Campos X., Young H. K., Husker A., Davis P., Clayton R., Iglesias A., Pacheco J., Singh S., Manea V., Gurnis M., 2008, Horizontal subduction and truncation of the Cocos Plate beneath central Mexico. *Geophysical Research Letters*, Vol. 35, L18303, DOI:10.1029/2008GL035127

Parzen E., 1960, Modern probability theory and its applications. J Wiley & Sons, Inc, Japan, 464pp.

Richter C., 1958, Elementary seismology. W H Freeman and Co, USA.

Scholz C., 1968, The frequency-magnitude relation of microfracturing in rock and its relation to earthquakes. *Bulletin of the Seismological Society of America*, 58:399–415

Shaw E., Carlson J. M., Langer J., 1992, Patterns of Seismic Activity Preceding Large Earthquakes. *Journal of Geophysical Research*, Vol. 97, No. B1, Pages 479-488.

Utsu T., 1965, A method for determining the value of b in a formula log n = a - bM showing the magnitude-frequency relation for earthquakes, *Geophysical Bulletin of the Hokkaido University*, 13, 99–103.

Utsu T., 1999, Representation and Analysis of the Earthquake Distribution: A Historical Review and Some New Approaches. *Pure and Applied Geophysiscs*, 155, 509-535.

Wyss M., Wiemer S., 2000, Change in the probability for earthquakes in southern California due to the Landers magnitude 7.3 earthquake. *Science*, Vol. 290, 1334

Zúñiga F. R., Reyes M. A., Valdés C. M., 2000, General overview of the catalog of recent seismicity compiled by the Mexican Seismological Survey. *Geofísica Internacional*. 39 (2), 161-170.